Energy Storage and Conversion 2024, 2(2), 1321.
https://doi.org/10.59400/esc.v2i2.1321

Article

Investigation of self-excited induction generator for supporting domestic loads and its extension to a microgrid

Arunava Chatterjee

Electrical Engineering Department, Raghunathpur Government Polytechnic, Purulia 723121, India; arunava7.ju@gmail.com

CITATION

Chatterjee A. Investigation of self-excited induction generator for supporting domestic loads and its extension to a microgrid. Energy Storage and Conversion. 2024; 2(2): 1321.
https://doi.org/10.59400/esc.v2i2.1321

ARTICLE INFO

Received: 2 April 2024
Accepted: 13 May 2024
Available online: 2 June 2024

Abstract: This study provides a technical and financial analysis for the incorporation of a microgrid structure with a wind energy conversion system for producing electricity. This study's primary aim is to provide solutions for issues that arise when isolated induction generators are employed with microgrids. A closed-loop smart electronic load controller is used to regulate the loads in the system that are supplied by the generator. A switched variable capacitor bank is used to supply reactive power initially during a voltage dip at varying winds and loads to sustain the voltage profile. Additionally, a simple voltage control loop-based controller for the generator-side converter maintains the voltage at a steady level. Using HOMER software, an economic study of the suggested wind-based microgrid structure is also presented. A laboratory experimental setup is used to support the MATLAB/Simulink study of the proposed method and its control. The findings support the feasibility of implementing the suggested plan in grid-isolated regions for supplying critical loads.

Keywords: induction generator; microgrid; smart electronic load controller; voltage regulation; wind power

1. Introduction

Nowadays, the mainstream of the energy used to generate electricity comes from the burning of fossil fuels like coal, oil, and natural gas. These fossil fuels have finite stocks, and burning them releases a significant amount of toxic gases into the atmosphere. Therefore, finding clean and sustainable sources of energy is always necessary. Wind is a pure and limitless renewable energy source. There are several ways to transform wind energy into electrical form, but using a wind turbine is by far the most common method [1]. In theory, any sort of generator may be installed atop a wind turbine to produce electricity. Even if the generator only produces direct current or alternating current with variable amplitude and frequency, the requirement for grid-compatible electric current may currently be satisfied by connecting appropriate converters.

With its robustness, minimal maintenance requirements, and easy controls, the induction generator (IG) seems to be an excellent option for these applications [2]. IG is preferred for producing wind energy due to its ease of use, dependability, and compact size per generated kilowatt. Moreover, IGs do not require an external power source to produce the excitation magnetic field. They can therefore be applied in far-off [3] and grid-isolated isolated locations [4]. The main limitations of IGs, however, are reactive power consumption and poor voltage regulation at variable speeds, although the invention of static power converters has made it easier to regulate the output voltage of IGs [5].

Because it does not require an external power source to generate the magnetic field, the self-excited induction generator (SEIG) is an excellent choice for wind-driven electric generation applications, particularly for variable wind speeds and isolated places. Although the SEIG scheme was discovered more than 80 years ago, a significant number of research publications have only recently become increasingly focused on the examination [6] and uses of SEIGs [7]. This is because voltage and frequency control techniques have advanced and because the development of renewable energy sources has received enormous global attention over the past thirty years.

The SEIG system's inability to regulate voltage and frequency under variable load situations is its primary operating issue. The machine excitation is immediately impacted by a change in the load impedance. This is because both the induction machine acting as a generator and the load impedance share the excitation capacitors' reactive power. As a result, when the load impedance is increased, the generator's voltage lowers, leading to poor voltage control. On the other hand, even though the speed of the prime mover is constant, the slip of the induction generator rises with increasing load, resulting in a frequency that depends on the load. Many studies have been conducted in the past to regulate the voltage and frequency of a SEIG system operating with variable loads. A high-cost speed governor is generally used as a conventional SEIG controller. A sliding mode controller was proposed, showing controlled dynamic response and behavior of the system upon changes in generator parameters and load [8]. Regulating the voltage and frequency of a SEIG under varying load conditions by an electronic load controller (ELC) was examined [9]. With the adoption of static converters, the voltage regulation problem is somewhat resolved [10], although the system cost has increased to a considerable extent [11]. Often, maximum power point tracking (MPPT)-based control techniques are adopted. Although various MPPT approaches make it easier to operate [12], especially in grid-connected generation [13], standalone grid-secluded generation is frequently controlled without MPPT to reduce the system complexity [14]. However, maintaining a constant generation becomes crucial since independent generations are frequently employed to handle important loads [15]. Hybrid energy storage-based microgrids with modified controls were recently studied for wind power generation [16]. The use of SEIG under unbalanced conditions has also been studied for power generation [17]. This method, although cheap, requires derating the machine, and thus IG operates with reduced capacity. Recent research for wind based renewable power generation focuses on control based on electric springs for flexible voltage control and wind power integration at the expense of cost and complexity [18,19]. Lowering the cost of electric spring-based microgrids is also attempted in the study of Mohanty et al. [20]. Although sometimes it is difficult to effectively regulate voltage for SEIGs without increasing the system cost and complexity.

This research includes a technical and economic analysis of the IG system when feeding varying domestic loads in an effort to aid in the resolution of the aforementioned operational issues with SEIGs. A dynamic capacitor-based voltage regulation scheme is proposed in the planned study, which is shown to be promising in providing variable reactive power initially during load and speed transients. A smart electronic load controller (SELC) is also proposed for load control, which is unique.

The transient response is observed to be better using a simple voltage loop-based converter control for the IG. The IG can then be connected to other renewable generating sources for providing continuous power to grid-isolated loads.

2. System description

The proposed generation system consists of a three-phase induction machine that is connected to a wind turbine for generation purposes. The IG is connected to a bus where system loads can also be connected for supply. To supply the initial reactive power, the stator windings of the induction machine are linked to a capacitor bank. The initial excitation is calculated from reactive power balancing [21]. For augmenting and supporting generation, the IG system can also be connected to a standby PV panel. A storage battery is also connected via a charge controller to support the loads during lean generation periods. The overall connected system is shown in **Figure 1**.

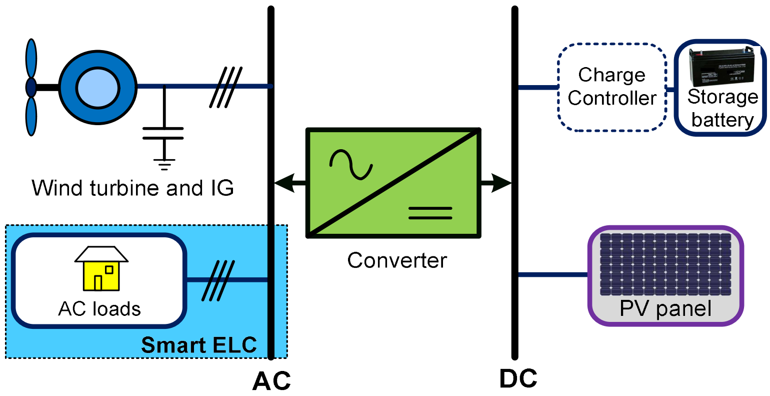

Figure 1. Block diagram of the wind-PV hybrid generation system.

The proposed system is envisioned to be used in a grid-isolated location in an onshore eastern Indian location. The location is not connected to a grid, and hence the utility of the proposed scheme of generation is of prime importance in supplying power to the remotely connected loads.

3. Proposed control scheme

The proposed system generation is provided using the IG. With the IG, a photovoltaic (PV) panel may also be connected. For the control, the microgrid structure with PV panels is not considered. The control is mainly focused on the IG side control of the smart electronic load controller (SELC) and the capacitor bank control with variable wind speeds and variable loads. The control scheme is shown in **Figure 2**. The SELC consists of an ESP-based Wi-Fi-enabled controller that can turn ON/OFF consumer loads based on the generated voltage and load requirements. This is done with the help of relay control, which is obtained using commands to be provided by the operator using the ESP board and a visual dashboard. The entire communication established with the load is done using the Internet of Things (IoT). Any communication protocol may be used, such as the popular message queuing telemetry transport (MQTT) [22] or data distribution system as in the study of

Chatterjee et al. [23]. Here, MQTT is used as it is lightweight and flexible for such control [24].

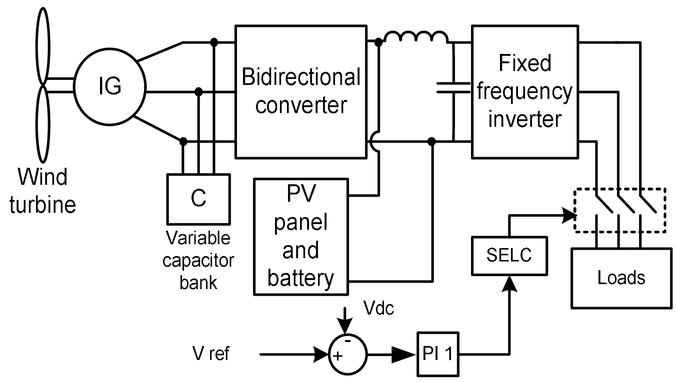

Figure 2. Block diagram of the control scheme for IG with loads.

For the proposed automatic load control, the DC bus voltage is sensed using a voltage sensor. The reference is compared, and the set error is sent to a proportional-integral controller (PI1). The output from the PI1 is taken as the reference data for sending it to SELC. The variable capacitors are controlled by load and speed parameters according to necessity. The SELC consists of an ESP8266-based controller. The operator is thus in a position to control the loads automatically using the sensed voltage data or can decide to turn ON/OFF loads as per requirement using the SELC controller.

4. Connection with microgrid

The IG-based generation system is to be connected with a microgrid, and its cost will also have to be estimated. The cost estimation and optimization are done using "HOMER" software [25]. HOMER Energy is the global standard for optimizing microgrid design in all sectors, from village power and island utilities to grid-connected campuses and military bases. Originally developed at the National Renewable Energy Laboratory and enhanced and distributed by HOMER Energy, HOMER (Hybrid Optimization Model for Multiple Energy Resources) nests three powerful tools in one software product, so that engineering and economics work side by side. HOMER is used because it can simplify and compare hundreds of alternatives to optimization in a single run. This also enables us to observe the effects of external factors, including wind speed and insolation, and comprehend the effect of fluctuations in the ideal system.

For the online microgrid simulation, some elements are used. The elements are an IG-based wind generator, a primary load, a converter, a battery, and a PV panel. There are two buses used. PV cells should be connected to a DC bus only. It is used only when the wind power is not enough to start the generator. A battery is also used there, with the DC bus as the backup source of power. The generator is connected to the AC bus only since it is an IG. A primary load is connected to an AC bus. The system simulation model is shown in **Figure 3**.

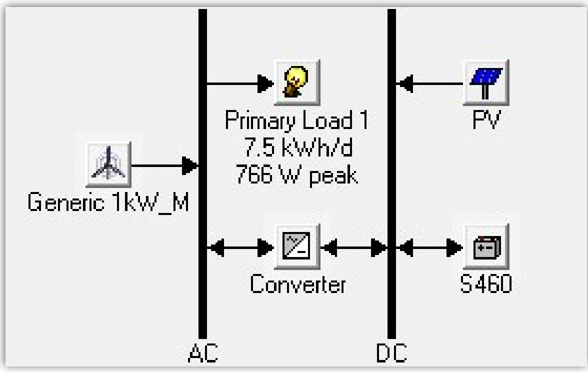

Figure 3. Simulation model of the proposed system.

The converter here is connected to both the AC and DC buses, as shown in **Figure 3**. After the connection is done, the results can be calculated and optimized with different numbers of iterations. The solar and wind data are obtained for the proposed place for setup using the NREL laboratory, as shown in **Figure 4**.

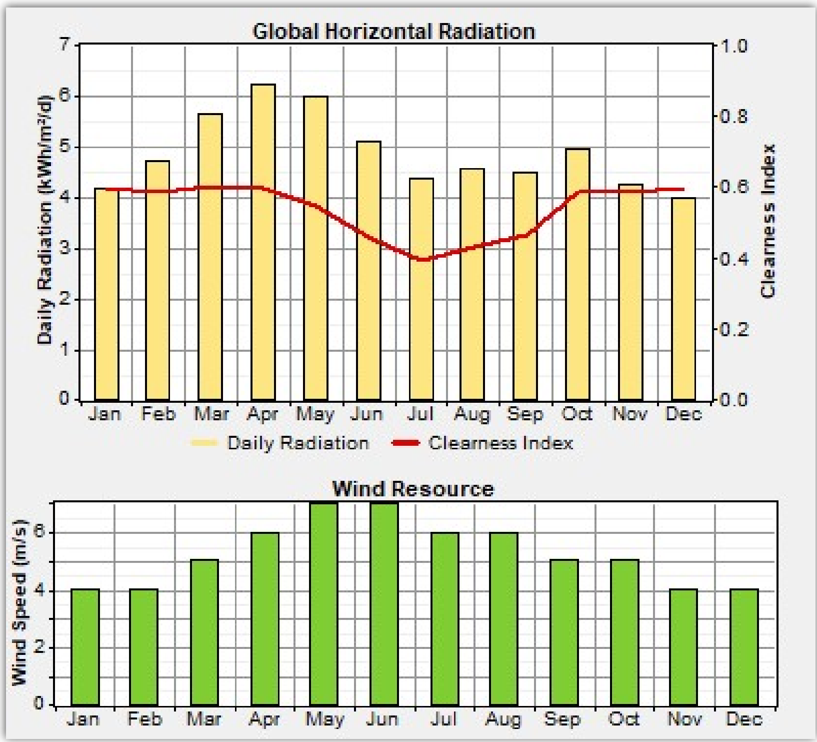

Figure 4. Solar radiation data and wind speed data variation for different months in a year for the installed place.

The PV module is employed when the availability of wind power is low, although it always remains connected to the system and surplus energy is stored in the battery. So, the PV module can supply loads in such cases. Whenever the wind power is low, the PV module provides the power, and whenever the PV module's power is low, the wind generates the power, as seen in **Figure 4**. It is concluded that the two powers complement each other for the proposed place of setup. The HOMER is used mainly to provide economic analysis along with technological support analysis. Therefore, using the software, the tabulated optimized cost output is shown in **Table 1**.

Table 1. Analysis of the proposed microgrid system with SEIG and PV support.

Initial capital ($)	Net present cost ($)	Operating cost ($/year)	Cost of energy ($/kwh)	Renewable fraction
4580	5350	105	0.158	1.00

The different optimized costs are assessed using the HOMER software when provided with the initial cost of the system components. These costs are verified using a market survey. With the 1 kW IG for the setup, two 500W-peak polycrystalline silicon PV panels are used. Both panels have a voltage rating of 48 V. Deep-cycle lead acid storage batteries with ratings of 12 V and 150 Ah of four numbers in series with overcharge/discharge protection are used for the connected system. The peak load is 760 W. The batteries offer a two-hour backup. The 22-A charge controller is used for charging purposes. The turbine-generator system costs about $3000, and replacing it will set you back $2500. Annually, the cost of operation and maintenance is estimated to be 2% of the original cost. The turbine is erected at a hub height of 10 m. The simulation uses a PV panel rated for 1 kW-peak, 48 V, with a capital cost of $1000 and 2% of the initial cost reserved for annual maintenance. The converter is rated at 1 kW, costs $300 in original capital, and requires $200 in replacement with zero maintenance annually. The battery costs $100 in capital when purchased, and it costs $50 to replace. Watering the battery is mostly covered by the $5 yearly operation and maintenance fee. The table provides the initial capital requirement after discounts, the net present cost of the system, and the operating cost of running such a system in a year. The different cost parameters are simulated and optimized in HOMER. To calculate the Net Present Cost (*NPC*) of the system, the discounted costs are typically deducted from the present values of the various power sources. Thus,

$$NPC = C_i + C_o + C_r - (C_e + C_s) \tag{1}$$

C_o is the system operation and maintenance cost, C_i is the initial system cost, C_r is the cost of system replacement, C_e and C_s are the sold surplus electricity cost and the salvaging cost of equipment at the end of total project life. The C_e value is calculated per hour and it is dependent on the load demand and power generated from the system. The value of C_r is calculated from the studies of Chatterjee and Banerjee [26], Dufo-López et al. [27] as,

$$C_r = \sum_{i=1}^{j} C_{r_k} \frac{(1+g_k)^{ij_k}}{(1+I_r)^{ij_k}} \tag{2}$$

where, C_{r_k} is cost of the replaced component, g_k is inflation rate and I_r is the rate of interest and j_k is total lifetime of *k*-th component. The value of C_s can be given as,

$$C_s = C_{r_k} \frac{R_c - (R_p - R_r)}{R_c} \tag{3}$$

where, R_c, R_p and R_r are respectively the individual component life, total project life and duration of replacement cost calculation. The cost of operation per year is the summation of running costs and other expenses which essentially exclude the initial cost of the system. The initial system cost C_i is given as,

$$C_i = C_{\mathrm{wtg}} P_{\mathrm{wtg}} + C_{\mathrm{pv}} P_{\mathrm{pv}} + C_{\mathrm{cnv}} P_{\mathrm{cnv}} + C_{\mathrm{bat}} P_{\mathrm{bat}} + C_c P_c \tag{4}$$

where *C* denotes unit cost and *P* denotes the nominal power of the sources of the wind turbine generator, PV panel, converters, and batteries, respectively. The C_c denotes the unit cost of the controller, and its nominal power is denoted as P_c which can be neglected. The various equations show that the *NPC* is a variable that may be tuned to reduce the overall cost of the system. The HOMER is used to do this task. The cost of energy (*COE*) is another metric that establishes the optimal net present cost. The ratio of the yearly cost of electricity production to the total electric load provided is used to determine this number. It is defined as,

$$COE = \frac{C_a}{E_s} \tag{5}$$

where total annualized cost of the proposed system is given as C_a (\$/yr) and the total load in terms of energy served is denoted as E_s (kWh/yr). It may be roughly understood as the *NPC* to total load supplied ratio.

It is estimated that the system is going to be used for a period of 25 years. By this time, the net present cost of the system can be mostly salvaged. The cost of generation from fossil fuels is around \$0.120 per kWh [28] to \$0.140 per kWh [29], which is also comparable with full renewable energy generation in the present case.

The cost of production of one unit of energy for such a system is shown to be lower, which is a definite advantage. Such a system, when connected to the grid, can thus supply power at a very cheap rate.

5. Results and discussion

The hardware implementation of the project is done in two parts. Firstly, the simulation results are tested using MATLAB/Simulink. It uses the preset models of the three-phase induction machine and other components. The IG model is considered to have a stationary reference frame and have the same parameters as the experimental machine. The hardware implementation is tested using a laboratory prototype. Secondly, a smart electronic load controller is designed for the proposed IG hardware setup.

The 3-phase induction machine operated as a generator is rated at 2 kW, 415 V, 50 Hz, and is wound for 4 stator poles. The machine parameters are provided in Appendix. The voltage generation initiates at a speed of 1150 rpm at no load without the proposed control (**Figure 2**). Although the speed is low for generation, the capacitor used reduces the operating point of the IG, and thus generation initiates at a lower speed. However, the generated voltage frequency at this speed is lower than 50 Hz. As the generator reaches a steady state, terminal loads across the main windings of the generator can be connected. The experimental setup, as shown in **Figure 5,** uses an induction machine coupled with a DC machine. The DC machine acts as a prime mover. The DC machine can be used to emulate wind turbine characteristics with some modifications. The generator-side bidirectional converter is controlled using a simple voltage loop-based proportional-integral (PI) controller. This controller is responsible for providing stable voltage output with load and speed transients. The voltage reference is taken as a dynamic function of the available wind speed (ω_r), which is compared with the generated voltage. The error is fed to the PI controller. The output of the PI controller is the current reference, which is used to generate pulses for the converter using hysteresis band-based control to sense the generator current. The PI controller is tuned using the Ziegler-Nichols method. Initially, the integral gain is set to zero, and the proportional gain is increased from zero until sustained oscillations are observed. This gain value and oscillation time are used to set the integral gain for minimal overshoot with judicious settling time. The controller is shown in **Figure 6**. The fixed-frequency inverter is operated at 50 Hz to supply the connected loads.

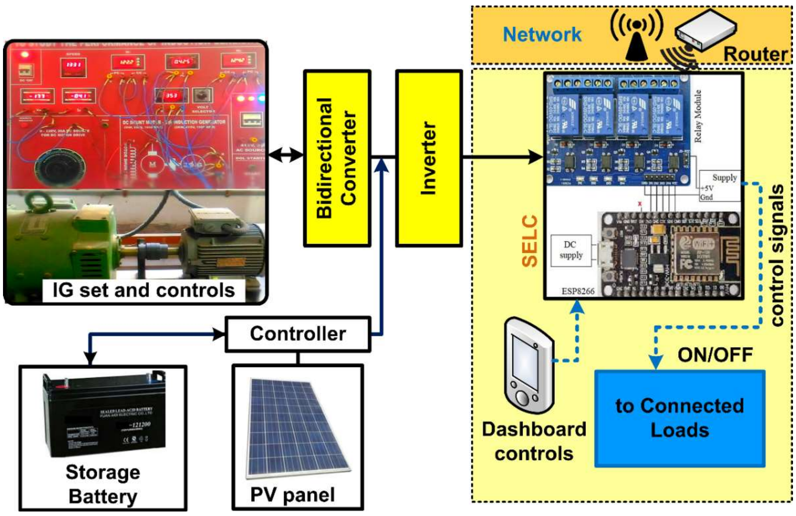

Figure 5. Experimental setup of the IG system with the smart electronic load controller.

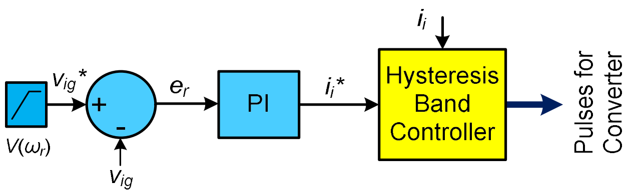

Figure 6. Controller for IG side converter.

However, it is assumed that the prime mover drives the generator at rated speed, considering that some gears may be used in real practice with the wind turbine to generate at rated speed for the IG. It was observed that the mechanical contacts of the laboratory-based experimental IG are competent enough for repeating use. This is due to mechanical wear and tear, and thus an electronic contactor switch was necessary. An ESP8266-controlled relay switch is developed for connecting the variable capacitors and loads. This is done using an electronic relay switch module. The connection of the relay coil for switching loads and capacitances makes the circuit better suited for the different loads and wind speed conditions. At first, the system is simulated using a three-phase induction machine model, which is used as IG in MATLAB/Simulink using a standard stationary frame model [30].

The simulated model has the same ratings as the proposed experimental setup. The proposed control is implemented for the simulated model. The generated voltage profile along with the change in wind speed is shown in **Figure 7**. With the proposed converter control, the voltage regulation is shown to be good with minimal change in voltage when the shaft speed is reduced by 200 r/min. Thus, with speed transients, the voltage is kept stable.

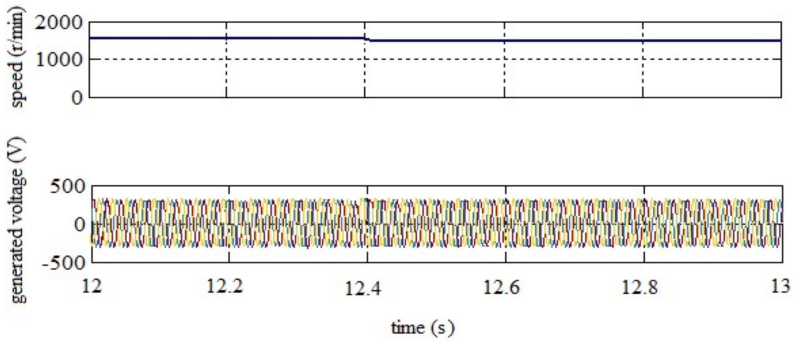

Figure 7. Simulated IG generated voltage with change in speed.

Next, the IG voltage variation with change in load from 1 A to 1.8 A at rated speed is done for the proposed control. It is observed that the generated voltage minimally changes with change in load. The same is shown in **Figure 8**. The load variation is done using the electronic load controller.

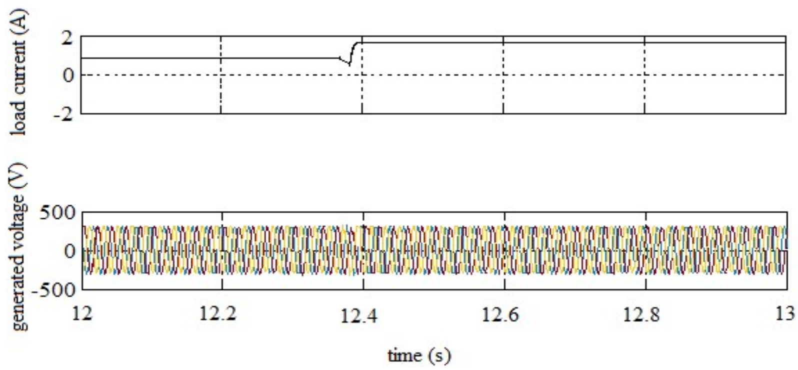

Figure 8. Simulated IG generated voltage with change in load.

The experimental waveforms for the proposed scheme are also shown. The generated voltage profile, along with a similar change in load and wind speed as that of the simulation study, are shown in **Figures 9a** and **9b,** respectively. It is observed that the simulation and experimental results are in good agreement.

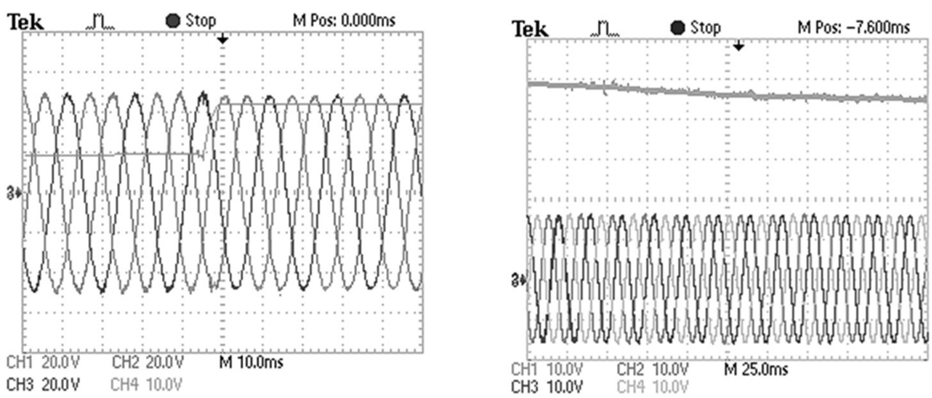

(a) **(b)**

Figure 9. Experimental IG generated voltage with change in **(a)** load (CH1, 2 and 3: *Y*-axis 200 V/div., CH4: *Y*-axis: 1 A/div.); and **(b)** speed (CH1: *Y*-axis: 300 r/min/div., CH2, 3 and 4: *Y*-axis: 200 V/div.).

The electronic load controller switching transients are observed experimentally. With a change in load, the observed waveform is shown in **Figure 10**. It is seen that the controller transients are minimal. The voltage regulation for such a change in load is shown in **Figure 9a**. The observed voltage regulation is better than most conventional control schemes. The load and speed transients are also better. Moreover, the cost and complexity of the scheme are also on the lower side, which are the added advantages.

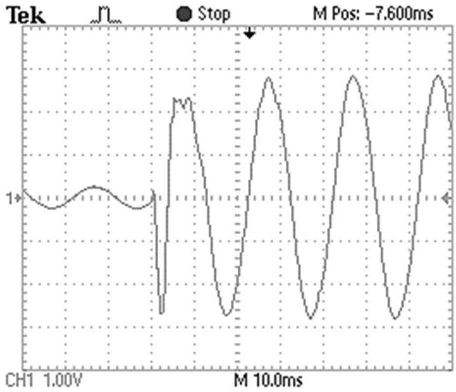

Figure 10. Experimental waveform for change in load in SELC.

6. Conclusion

This research presents a technical and economic analysis of a wind energy conversion system and its integration into a microgrid structure for isolated electricity generation. The modeling is done in HOMER software, which provides the platform to simulate the economic viability of the scheme. The cost of generation obtained is comparable to conventional generation with less system complexity. The bidirectional converter control helps to provide stable voltage with an active voltage control loop. The smart electronic load controller also helps to provide flexible switching of loads with minimal transients for load control.

The characteristics of the SEIG and its proposed control are studied in a MATLAB/Simulink environment and later validated with a laboratory experimental prototype. It is found to be a viable solution for providing power to a remote location. With even proper cost details, the accuracy of the cost optimization can be increased. Moreover, some meta-heuristic or artificial intelligence-based optimization techniques can also be applied for further improved results.

In the future, suitable design procedures with further optimizations for the IG can be implemented. Further, the study of grid integration of the IG with the proposed controller can be a scope of research, and its performance improvement study can also be considered.

Conflict of interest: The author declares no conflict of interest.

References

1. Patel MR, Beik O. Wind and Solar Power Systems, 3rd ed. CRC Press; 2021.
2. Chojaa H. A novel DPC approach for DFIG-based variable speed wind power systems using DSpace. IEEE Access. 2023; 11: 9493-9510. doi: 10.1109/access.2023.3237511

3. Faisal Khan M, Khan M, Iqbal A. Effects of induction machine parameters on its performance as a standalone self-excited induction generator. Energy Reports. 2022; 8: 2302-2313. doi: 10.1016/j.egyr.2022.01.023
4. Grgic I, Basic M, Vukadinovic D, et al. Optimal control of a standalone wind-solar-battery power system with a quasi-z-source inverter. In: Proceedings of the 2020 9th International Conference on Renewable Energy Research and Application (ICRERA); 27-30 September 2020; Glasgow, UK. pp. 61-66. doi: 10.1109/ICRERA49962.2020.9242854
5. Hamid B, Hussain I, Iqbal SJ, et al. Optimal MPPT and BES Control for Grid-Tied DFIG-Based Wind Energy Conversion System. IEEE Transactions on Industry Applications. 2022; 58(6): 7966-7977. doi: 10.1109/tia.2022.3202757
6. Ion CP. A Comprehensive Overview of Single–Phase Self-Excited Induction Generators. IEEE Access. 2020; 8: 197420-197430. doi: 10.1109/access.2020.3034291
7. Chatterjee A, Chatterjee D. PV-assisted microgeneration scheme with single-phase induction generator suitable for wide speed range application. IET Power Electronics. 2017; 10(14): 1859-1869. doi: 10.1049/iet-pel.2016.0535
8. Mi Y, Song Y, Fu Y, et al. The Adaptive Sliding Mode Reactive Power Control Strategy for Wind–Diesel Power System Based on Sliding Mode Observer. IEEE Transactions on Sustainable Energy. 2020; 11(4): 2241-2251. doi: 10.1109/tste.2019.2952142
9. Singh S, Azad ML, Kumar A. Electronic load controllers for self-excited induction generator. In: Proceedings of the 2016 International Conference on Innovation and Challenges in Cyber Security (ICICCS-INBUSH); 3-5 February 2016; Greater Noida, India. pp. 300-303. doi: 10.1109/ICICCS.2016.7542354
10. Chatterjee A. Analysis of a Wind-PV hybrid system with smart control for grid-secluded critical loads in onshore Indian area. In: Bhaumik S, Chattopadhyay S, Chattopadhyay T, Bhattacharya S (editors). Proceedings of International Conference on Industrial Instrumentation and Control (ICI2C 2021); 20-22 August 2021; Kolkata, India. Springer; 2022. pp. 495-503. doi: 10.1007/978-981-16-7011-4_47
11. Chatterjee A. Wind-PV based generation with smart control suitable for grid-isolated critical loads in onshore India. Journal of The Institution of Engineers (India): Series B. 2022; 52: 1-11. doi: 10.1007/s40031-022-00827-2
12. Huynh P, Tungare S, Banerjee A. Maximum Power Point Tracking for Wind Turbine Using Integrated Generator–Rectifier Systems. IEEE Transactions on Power Electronics. 2021; 36(1): 504-512. doi: 10.1109/tpel.2020.3002254
13. Shutari H, Ibrahim T, Mohd Nor NB, et al. Development of a Novel Efficient Maximum Power Extraction Technique for Grid-Tied VSWT System. IEEE Access. 2022; 10: 101922-101935. doi: 10.1109/access.2022.3208583
14. Roy K, Chatterjee A, Chatterjee D, et al. A Photovoltaic-based Improved Excitation Control Strategy of Three-phase Self-excited Induction Generator Suitable for Wind Power Generation. Electric Power Components and Systems. 2015; 43(17): 1912-1920. doi: 10.1080/15325008.2015.1070382
15. Chatterjee A, Ghosh S, Mitra A. Wind-PV based isolated hybrid generation for smart irrigation management and supplying other critical loads. In: Proceedings of the 2022 IEEE 2nd International Conference on Sustainable Energy and Future Electric Transportation (SeFeT); 4-6 August 2022; Hyderabad, India. pp. 1-6. doi: 10.1109/SeFeT55524.2022.9908711
16. Behera PK, Pattnaik M. Coordinated Power Management of a Laboratory Scale Wind Energy Assisted LVDC Microgrid With Hybrid Energy Storage System. IEEE Transactions on Consumer Electronics. 2023; 69(3): 467-477. doi: 10.1109/tce.2023.3287099
17. Liu Y, Masadeh MA, Pillay P. Power-Hardware-In-The-Loop-Based Emulation of a Self-Excited Induction Generator Under Unbalanced Conditions. IEEE Transactions on Industry Applications. 2022; 58(1): 588-598. doi: 10.1109/tia.2021.3118985
18. Panda D, Kundu P, Rajpuroit BS. Real-time voltage control and harmonics elimination of islanded microgrid using back-to-back electric spring. IEEE Transactions on Industry Applications. 2024. doi: 10.1109/TIA.2024.3397963
19. Mohanty S, Pati S, Kar SK, et al. A Novel Electric Spring with Improved Range of Operation for Isolated Microgrid Systems. IEEE Access. 2023; 11: 75761-75781. doi: 10.1109/access.2023.3295888
20. Mohanty S, Pati S, Kumar Kar S. Improved islanded microgrid performance with sliding mode controller based electric spring. Renewable Energy Focus. 2024; 48: 100535. doi: 10.1016/j.ref.2023.100535
21. Trzynadlowski A. Control of Induction Motors, 1st ed. Academic Press; 2001.
22. Ghosh S, Chatterjee A, Chatterjee D. Extraction of statistical features for type-2 fuzzy NILM with IoT enabled control in a smart home. Expert Systems with Applications. 2023; 212: 118750. doi: 10.1016/j.eswa.2022.118750
23. Chatterjee A, Ghosh S, Mitra A. Hybrid generation scheme for delivering irrigation loads and other critical loads with smart IoT based control. IEEE Transactions on Industry Applications. 2024; 60(1): 828-837. doi: 10.1109/TIA.2023.3322114
24. Ganguly B, Chatterjee A. MQTT protocol based extensive smart motor control for electric vehicular application. In:

Proceedings of the 2020 IEEE 7th Uttar Pradesh Section International Conference on Electrical, Electronics and Computer Engineering (UPCON); 27-29 November 2020; Prayagraj, India. pp. 1-5. doi: 10.1109/UPCON50219.2020.9376452
25. Homer Energy. Available online: https://www.homerenergy.com/ (accessed on 17 April 2024).
26. Chatterjee A, Banerjee B. Cost-Effective Hybrid Wind-Photovoltaic Generation System for Isolated Critical Loads: A Case Study. Journal of Electronics and Electrical Engineering. 2023. doi: 10.37256/jeee.2220233735
27. Dufo-López R, Bernal-Agustín JL, Mendoza F. Design and economical analysis of hybrid PV–wind systems connected to the grid for the intermittent production of hydrogen. Energy Policy. 2009; 37(8): 3082-3095. doi: 10.1016/j.enpol.2009.03.059
28. Global Petrol Prices. Available online: https://www.globalpetrolprices.com/India/electricity_prices/ (accessed on 17 April 2024).
29. Strielkowski W. Renewable energy sources, power markets, and smart grids. In: Social Impacts of Smart Grids, 1st ed. Elsevier; 2020. pp. 97-151.
30. Bose BK. Modern Power Electronics and AC Drives, 1st ed. Prentice Hall; 2001.

Appendix

Table A1. Induction machine parameters.

Parameters	**Values per phase**
Stator circuit resistance	6.44 Ω
Rotor circuit resistance	6.57 Ω
Stator and rotor leakage inductance	8.55 mH
Magnetising inductance	276.55 mH
Inertia constant	0.142 kg·m^2